

Improvements for BLDC motor control

Martin Dodek*, Eva Miklovičová*

* Faculty of Electrical Engineering and Information Technology Slovak University of Technology in Bratislava
Email: *martin.dodek@stuba.sk, eva.miklovicova@stuba.sk*

Abstract—In this paper we address some novel modifications of commonly used algorithms and techniques related to the problem of sensor-less field-oriented control (abbr. FOC) of brushless DC (abbr. BLDC) motors. The most significant outcome of this research is design of an innovative procedure for motor parameters identification - performable directly in the target application without using any additional equipment. This makes possible to control a motor with initially unknown parameters, thereby yielding the ability to apply the “plug and play” concept. In addition, the essential operation of the vector-rotation was treated in a new way - using the Taylor series approximation. We marginally focused on the inverter voltage modulation algorithm where we proposed its simple yet very effective implementation. The structure and parameters design of the rotor position estimator were rigorously derived - based on the Luenberger observer. The original algorithm of the field-oriented control was modified by using current controllers with the IP structure. Physical constraints of the manipulated variable reflected into using the anti-windup algorithm. Here we introduced a special ability to tune the saturation levels for both components of the controlled current individually. Finally, a real-motor identification and control experiment was carried out in order to validate all the proposed improvements and modifications.

Index Terms—field-oriented control, BLDC motor, SVPWM, BEMF observer, PLL, system identification, embedded systems

I. INTRODUCTION

In the last decade, even more applications of various actuators systems relies on the brushless DC motors technology. Besides the industrial applications also consumer-oriented products e.g. e-bikes or drones are widely utilizing BLDC motors nowadays. Yet there are still many problems that need to be solved and possible improvements that can be done in this field.

The brushless DC motor is a synchronous three-phase machine with permanent magnet rotor construction. These motors are typically numerically controlled by a micro-controller and powered by a transistor-based bridge inverter.

A. Coordinate systems

For the mathematical description of the BLDC motor - special coordinate systems have to be used. A general three-phase vector comprises three separate components for each phase:

$$v_{abc} = [v_a, v_b, v_c] \quad (1)$$

However, the motor model as well as the field-oriented control algorithm itself are both using an equivalent two-phase coordinate system.

$$v_{xy} = [v_x, v_y] \quad (2)$$

Where the x component can be treated as the real while the y component as the imaginary part of a complex number.

In order to transform a three-phase to the equivalent two-phase vector the $3/2$ transform, also known as the Clarke¹ transform, can be used. Similarly, the back-transform of vectors can be performed using the $2/3$ transform, also known as the inverse Clarke transform. Although these transforms are an essential part of the control algorithm (see figure 5), they are not in the primary scope of this paper.

B. Park transform (and inverse)

Concerning the used coordinate systems - there are two reference frames mutually rotated by the angular position ϕ . Specifically there is the fixed stator $\alpha\beta$ and the rotor dq reference frame.

The Park transform represents a vector rotation operation defined by the complex exponential function.

$$v_{\alpha\beta} = v_{dq} e^{j\phi} \quad (3)$$

For the component representation of a vector, the Park transform can be written in the matrix form:

$$\begin{pmatrix} v_\alpha \\ v_\beta \end{pmatrix} = \begin{pmatrix} \cos(\phi) & -\sin(\phi) \\ \sin(\phi) & \cos(\phi) \end{pmatrix} \begin{pmatrix} v_d \\ v_q \end{pmatrix} \quad (4)$$

On the contrary, the inverse Park transform is equal to the negative angle rotation operation:

$$v_{dq} = v_{\alpha\beta} e^{-j\phi} \quad (5)$$

The equivalent matrix representation of the equation (5) can be derived as the matrix inverse of (4). Notice, that matrix (4) is orthogonal so it's inverse is simply equal to the transposed matrix.

II. TRIGONOMETRIC FUNCTIONS APPROXIMATIONS

Trigonometric functions *sine* and *cosine*, as a part of the Park transform matrix (4), are evaluated multiple times for each iteration of the control algorithm. Direct using of the standard math library implementation of these functions is therefore considered as a significant bottleneck.

One possible way of achieving the necessary performance boost is using lookup tables. Since all the pre-computed values have to be stored, the significant memory occupation is the main drawback of the lookup tables.

¹Named after Edith Clarke

A. Taylor series expansion

An alternative way of approximating the trigonometric functions is the Taylor series expansion. The n th-order series expansion of the *sine* function around the point $x_0 = 0$ can be written as:

$$\sin(x) \approx p_0(x) = \sum_{k=0}^n (-1)^k \frac{x^{2k+1}}{(2k+1)!} \quad (6)$$

Assuming the $x_0 = \frac{\pi}{2}$ one can write:

$$\sin(x) \approx p_{\frac{\pi}{2}}(x) = 1 + \sum_{k=1}^n (-1)^k \frac{(x - \frac{\pi}{2})^{2k}}{(2k)!} \quad (7)$$

However, the Taylor series expansion is valid only for arguments in the neighbourhood of the assumed point x_0 . Therefore we proposed to combine both series (6),(7) into one function. The weighting provides high accuracy around both points of $0, \frac{\pi}{2}$, and satisfactory approximation error for the arguments in-between them.

$$\sin(x) \approx p_w = \left(1 - \frac{2}{\pi}x\right) p_0(x) + \frac{2}{\pi}x p_{\frac{\pi}{2}}(x) \quad (8)$$

The minimum yet quite usable series order was determined as: $n = 4$. The comparison of approximation errors for all the assumed variants can be seen in the figure 1.

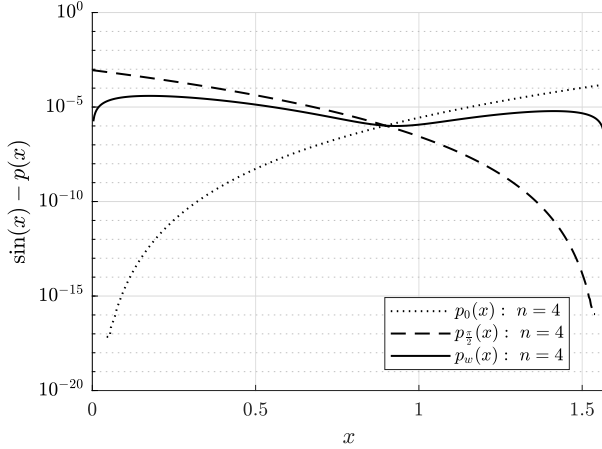


Fig. 1: Sine function Taylor series approximation error

For $x \notin \langle 0, \frac{\pi}{2} \rangle$, trigonometric properties of periodicity and symmetry can be used conveniently.

$$\begin{aligned} \sin(x) &= \sin(x + 2\pi k) & k = 1, 2 \dots n \\ \sin(x) &= -\sin(x - \pi) & \pi < x < 2\pi \\ \sin(x) &= \sin(\pi - x) & \frac{\pi}{2} < x < \pi \end{aligned} \quad (9)$$

Identities for negative argument and *sine-cosine* relation can be also assumed:

$$\begin{aligned} \sin(-x) &= -\sin(x) \\ \cos(x) &= \sin(x + \frac{\pi}{2}) \end{aligned} \quad (10)$$

However, choosing either a lookup table or a Taylor series is always trade-off between computational complexity and memory requirements.

III. MODEL OF THE BLDC MOTOR

In this section, dynamic models of the BLDC motor for dq and $\alpha\beta$ reference frame are briefly presented.

A. Model in the dq reference frame

Assuming the dq reference frame, all the concerned variables are represented from the rotor point of view i.e. linked to the shaft mechanical rotation.

The BLDC motor model for the dq reference frame is presented bellow [1]:

$$u_d = Ri_d + L_d \frac{di_d}{dt} + \omega L_q i_q \quad (11)$$

$$u_q = Ri_q + L_q \frac{di_q}{dt} - \omega (L_d i_d + \psi_f) \quad (12)$$

Where the direct u_d and the quadrature u_q stator voltages represent the manipulated variables. The $L_d [H]$ and $L_q [H]$ parameters stand for the direct and the quadrature inductances of the winding and the $R [\Omega]$ parameter denotes the winding resistance. The permanent magnet flux is represented by the $\psi_f [Vs]$ parameter.

The torque generated by the motor can be written as:

$$M = \frac{3}{2}p(\psi_f i_q + (L_d - L_q) i_d) \quad (13)$$

Where the parameter p is the number of pole pairs.

B. Model in the $\alpha\beta$ reference frame

It is necessary to express the motor model also for the $\alpha\beta$ reference frame. Here, all the concerned variables are represented from the stator point of view i.e. are linked to the fixed body of the motor.

Dynamic equations for the α and β axis of the stator current are defined as follows [2]:

$$u_\alpha = Ri_\alpha + L_d \frac{di_\alpha}{dt} + \omega (L_d - L_q) i_\beta + E_\alpha \quad (14)$$

$$u_\beta = Ri_\beta + L_d \frac{di_\beta}{dt} - \omega (L_d - L_q) i_\alpha + E_\beta \quad (15)$$

The $E [V]$ vector denotes the *back electromotive force* signal (abbr. BEMF) that represents the induced harmonic voltage. The BEMF voltage signal is related to the rotor angular position ϕ and speed ω :

$$E_\alpha = -\sin(\phi) \left[(L_d - L_q) \left(\omega i_d - \frac{di_q}{dt} \right) + \omega \psi_f \right] \quad (16)$$

$$E_\beta = +\cos(\phi) \left[(L_d - L_q) \left(\omega i_d - \frac{di_q}{dt} \right) + \omega \psi_f \right] \quad (17)$$

In the case of a non-salient rotor i.e. $L_d = L_q$, there is possible simplification:

$$\begin{aligned} E_\alpha &= -\sin(\phi) \omega \psi_f \\ E_\beta &= +\cos(\phi) \omega \psi_f \end{aligned} \quad (18)$$

So the magnitude of the BEMF signal is proportional to the angular speed ω .

$$\|E\| = |\omega| \psi_f \quad (19)$$

IV. FIELD-ORIENTED CONTROL

The field-oriented control represents a method for independent control of the direct and the quadrature axis current-components. Thereby it is possible to manage the generated torque and the magnetic flux while maximizing the overall energetic efficiency.

Accordingly, the traditional FOC structure comprises two controllers (usually PI) for each of the i_d and i_q currents.

The FOC algorithm is supposed to hold the direct axis current as low as possible i.e. $i_{d_w} = 0$, whereas the quadrature axis current has to be kept at the reference value i.e. $i_{q_w} \neq 0$ - usually calculated by the superior control loop.

A. Control decoupling

Since the differential equations (11),(12) contain cross-coupling, to achieve independent control of both components, the decoupling algorithm has to be applied:

$$\bar{u}_d = u_d - \omega L_q i_q \quad (20)$$

$$\bar{u}_q = u_q + \omega L_d i_d \quad (21)$$

Moreover, by applying the above equation to the voltage vector, the controlled system (11),(12) can be even considered linear.

$$u_d = R i_d + L_d \frac{d i_d}{dt} \quad (22)$$

$$u_q = R i_q + L_q \frac{d i_q}{dt} - \omega \psi_f \quad (23)$$

B. IP controller

The IP controller is a structural modification of the PI controller where instead of single input for the error signal $e(t)$, both error and feedback $y(t)$ signals are provided.

$$u(s) = K_i \frac{1}{s} e(s) - K_p y(s) \quad (24)$$

The K_p and K_i parameters stand for the gain of the proportional and the integral term respectively.

Our motivation for introducing the IP controller rather than using the original PI structure was to eliminate the presence of zero i.e. numerator polynomial root in the resulting closed control loop transfer function.

C. Control synthesis

General aim of the controller parameters synthesis is to achieve desired dynamic behaviour of the closed control loop while implicitly providing it's stability. The design of the FOC IP controllers can be conveniently performed using the pole-placement method.

As a consequence of the control decoupling (20),(21), one can apply the Laplace transform to the differential equations (22),(23) while assuming the signal of angular speed ω as the external disturbance. This leads to the transfer function model of the controlled system in the following form:

$$i_d(s) = u_d(s) \frac{1}{(L_d s + R)} \quad (25)$$

$$i_q(s) = u_q(s) \frac{1}{(L_q s + R)} + \omega(s) \frac{\psi_f}{(L_q s + R)} \quad (26)$$

Then, the transfer function of the closed loop for the controller (24) and the plant (25),(26) takes the following form:

$$\frac{i_{d/q}(s)}{i_{w_{d/q}}(s)} = \frac{K_{i_{d/q}} + K_{p_{d/q}} s}{L_{d/q} s^2 + (R + K_{p_{d/q}}) s + K_{i_{d/q}}} \quad (27)$$

The stricken-through expression in this equation represents the difference between using the IP or the PI controller structure.

The desired characteristic polynomial can be in a second order aperiodic form, assuming the time constants $T_{1,2}$ [s]:

$$P(s) = (T_1 s + 1) (T_2 s + 1) \quad (28)$$

Finally, the parameters of the controller can be determined as:

$$K_{i_{d/q}} = \frac{L_{d/q}}{T_1 T_2} \quad (29)$$

$$K_{p_{d/q}} = L_{d/q} \frac{(T_1 + T_2)}{T_1 T_2} - R \quad (30)$$

D. Anti-windup algorithm

Because the manipulated variable i.e. stator voltage u_{dq} is physically constrained, the anti-windup algorithm has to be applied. This allows to avoid of an uncontrollable raise of the integrator output caused by the uncorrected saturation of the manipulated variable i.e. wind-up effect.

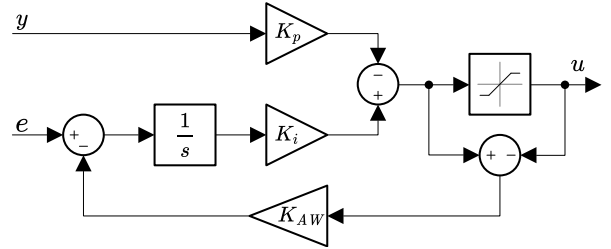


Fig. 2: Anti-windup modification of IP controller

For this algorithm to work correctly, the values of saturation have to be known exactly. The inequality for magnitude of the u_{dq} vector can be determined according to the applied supply voltage U_{DC} and regarding the properties of the SVPWM algorithm (see section VI) as:

$$u_d^2 + u_q^2 \leq \left(\frac{U_{DC}}{\sqrt{3}} \right)^2 \quad (31)$$

Therefore we can choose the maximum and the minimum values of the voltage components individually:

$$u_q^{max} = \gamma \frac{U_{DC}}{\sqrt{3}} \quad (32)$$

$$u_d^{max} = \delta \frac{U_{DC}}{\sqrt{3}} \quad (33)$$

$$u_{d/q}^{min} = -u_{d/q}^{max} \quad (34)$$

Where γ and δ are weights for the direct and the quadrature components respectively. However, these weights must meet the following inequality condition:

$$\gamma^2 + \delta^2 \leq 1 \quad (35)$$

This proposed modification allows to reflect the application-specific demands e.g. greater dynamic range for the quadrature current directly into the control algorithm.

V. SENSOR-LESS SOLUTION

In order to apply the FOC algorithm, the rotor angular position ϕ has to be sensed or at least estimated. A standard way to obtain this information is using an incremental rotary encoder, what usually requires an additional hardware sensor to be mounted on the rotor shaft. A sensor-less solution bypasses this hardware modification by indirect estimate of the rotor position ϕ from other available signals (stator currents).

A. BEMF observer

In this paper a Luenberger state observer is proposed for the purpose of the BEMF signal (18) estimation [3].

$$\dot{\hat{x}} = A\hat{x} + Bu + G(y - \hat{y}) \quad (36)$$

Where G denotes the Luenberger gain, being subject of the observer design. Concerning the time derivative of the estimate error $e = x - \hat{x}$, the following equation is important:

$$\dot{e} = (A - GC)e \quad (37)$$

The state-space representation of the stator winding model in the $\alpha\beta$ reference frame can be derived from the differential equations (14),(15) assuming non-salient rotor i.e. $L_d = L_q$ simplification.

$$x = \begin{bmatrix} i_{\alpha/\beta} \\ E_{\alpha/\beta} \end{bmatrix} \quad A = \begin{pmatrix} -\frac{R}{L_d} & -\frac{1}{L_d} \\ 0 & 0 \end{pmatrix} \quad B = \begin{pmatrix} \frac{1}{L_d} \\ 0 \end{pmatrix} \quad C = \begin{pmatrix} 1 \\ 0 \end{pmatrix}^T \quad (38)$$

The observer takes the form then:

$$\begin{bmatrix} \dot{\hat{i}}_{\alpha/\beta} \\ \dot{\hat{E}}_{\alpha/\beta} \end{bmatrix} = \begin{pmatrix} -\frac{R}{L_d} & -\frac{1}{L_d} \\ 0 & 0 \end{pmatrix} \begin{bmatrix} \hat{i}_{\alpha/\beta} \\ \hat{E}_{\alpha/\beta} \end{bmatrix} + \begin{pmatrix} \frac{1}{L_d} \\ 0 \end{pmatrix} u_{\alpha/\beta} + \begin{bmatrix} g_1 \\ g_2 \end{bmatrix} (i_{\alpha/\beta} - \hat{i}_{\alpha/\beta}) \quad (39)$$

The estimated state vector comprises the signal of the stator current estimate \hat{i} (either α or β component) and the BEMF signal estimate \hat{E} (also for separate components).

1) *Observer design:* The aim of the observer design is to provide convergence of the state estimate by placing appropriate eigenvalues of the estimate error feedback matrix (37).

The characteristic polynomial of the system (37) can be determined as [3]:

$$Q(s) = \det(sI - (A - GC)) \quad (40)$$

By substituting (38) into (40) we obtain the characteristic polynomial in explicit form:

$$Q(s) = \det \begin{pmatrix} s + \frac{R}{L_d} + g_1 & \frac{1}{L_d} \\ g_2 & s \end{pmatrix} \quad (41)$$

$$Q(s) = s^2 + \left(\frac{R}{L_d} + g_1 \right) s - \frac{g_2}{L_d}$$

The desired eigenvalues $\lambda_{1,2}$ form the desired characteristic polynomial $P(s)$:

$$P(s) = (s - \lambda_1)(s - \lambda_2) \quad (42)$$

By demanding the equality of $Q(s) = P(s)$ one can finally derive the observer gains.

$$g_1 = -\lambda_1 - \lambda_2 - \frac{R}{L_d} \quad g_2 = -\lambda_1 \lambda_2 L_d \quad (43)$$

B. Phase-locked loop

Since the BEMF signal vector, as defined in (18), contains the information of current angular position ϕ , it is therefore possible for this information to be extracted out. A simple and intuitive solution for doing so is using the *arctangent* function, although this operation is considered as noise sensitive and also introduces an adverse discontinuity.

To overcome this issue, the *phase locked loop* (abbr. PLL) can be exploited. The PLL is non-linear dynamic system used for tracking of the phase of a harmonic signal.

The non-linear feedback of this structure is designed to provide the phase estimate error signal e_ϕ (see equation (18)):

$$e_\phi = -E_\alpha \cos(\hat{\phi}) - E_\beta \sin(\hat{\phi}) = \omega \psi_f \sin(\phi - \hat{\phi}) \quad (44)$$

To provide an angular speed-independent dynamic behaviour of the PLL, normalization of the BEMF signal is necessary [2].

$$\bar{E} = \frac{E}{\|E\|} \quad (45)$$

Applying the equation (45) and substituting the BEMF magnitude (19), the PLL position estimate error (44) becomes:

$$e_\phi = \sin(\phi - \hat{\phi}) \quad (46)$$

The assumed model structure is a simple integrator $\dot{\phi} = \omega$.

So we can use the Luenberger state observer to estimate the angular speed $\hat{\omega}$ and the position $\hat{\phi}$:

$$\begin{bmatrix} \dot{\hat{\omega}} \\ \dot{\hat{\phi}} \end{bmatrix} = \begin{pmatrix} 0 & 0 \\ 1 & 0 \end{pmatrix} \begin{bmatrix} \hat{\omega} \\ \hat{\phi} \end{bmatrix} + \begin{bmatrix} g_1^{PLL} \\ g_2^{PLL} \end{bmatrix} (\phi - \hat{\phi}) \quad (47)$$

The resulting block diagram of the derived PLL structure is shown in the figure 3.

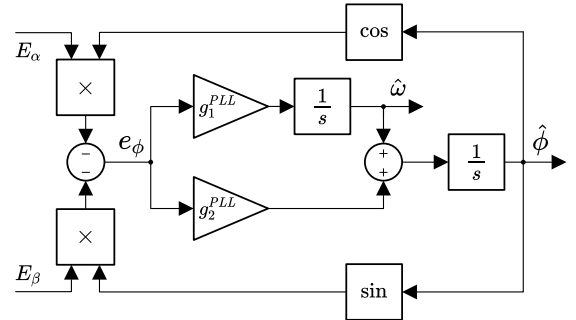


Fig. 3: PLL with Luenberger observer

One can also see the similarity between this observer structure and the PI-like estimator presented in [4] and [2].

For the PLL parameters design we have to determine the characteristic polynomial of the estimate error according to the equation (40):

$$Q(s) = \det \begin{pmatrix} s & g_1^{PLL} \\ -1 & s + g_2^{PLL} \end{pmatrix} \quad (48)$$

$$Q(s) = s^2 + g_2^{PLL}s + g_1^{PLL}$$

The desired characteristic polynomial $P(s)$, is in the same form as in the equation (42).

So by demanding equality of the characteristic polynomial (48) and the desired one (42), we can finally derive the observer gains as :

$$g_1^{PLL} = \lambda_1^{PLL} \lambda_2^{PLL} \quad g_2^{PLL} = -\lambda_1^{PLL} - \lambda_2^{PLL} \quad (49)$$

The phase portrait of the PLL can be seen in the figure 4.

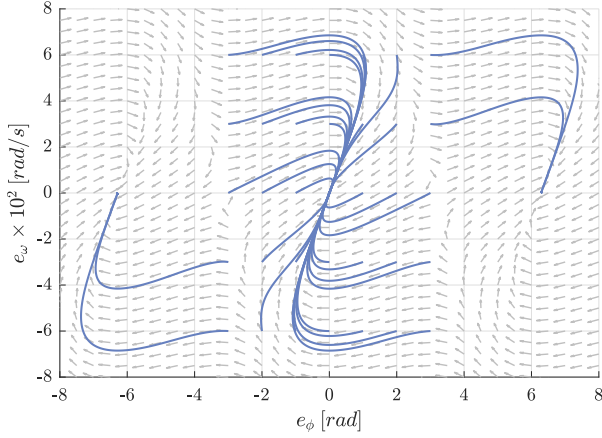


Fig. 4: Phase portrait of the PLL

VI. SPACE VECTOR PULSE WIDTH MODULATION

If the BLDC motor is powered by a three-phase transistor inverter, the technique called: *space vector pulse width modulation* (abbr. SVPWM) has to be applied in order to calculate the PWM duty vector d_{abc} from the provided voltage vector u_{abc} .

If not treated prudently - implementation of this algorithm may lead to significant consumption of the precious CPU time. Therefore we proposed a simple algorithm using the min function as possible substitute to the traditional solution.

A. SVPWM Min algorithm

This algorithm is not commonly used, yet it was already published e.g. in [5], [6] and references therein.

First we have to determine the neutral voltage u_N :

$$u_N = \min \{u_a, u_b, u_c\} \quad (50)$$

The duty vector d_{abc} for the provided supply voltage U_{DC} can be obtained as:

$$d_{abc} = \frac{u_{abc} - u_N}{U_{DC}} \quad (51)$$

Notice, that for every possible voltage vector, one of the duty components $d_{a/b/c}$ will always be zero using this method. This phenomenon is truly convenient, primarily because of the minimized transistors switching losses.

Since the PWM duty is inherently bounded to the interval $d_{a/b/c} \in \langle 0, 1 \rangle$ the magnitude of transformed voltage signal is allowed to be maximally (without the proof) $\frac{U_{DC}}{\sqrt{3}}$. It's also worth noting, that the requirement for all the duty signal components $d_{a/b/c}$ to be non-negative is always met.

Duty signals generated from the three-phase sinusoidal signal with amplitude of 2.5V using the SVPWM Min algorithm and assuming the supply voltage $U_{DC} = 5.0V$ is depicted in the figure 6.

VII. PARAMETERS IDENTIFICATION

In order to achieve optimal performance of the sensorless field-oriented control algorithm, the concerned motor parameters have to be known. Manufacturing processes of BLDC motors may lead to significant deviations in parameters so available data-sheet informations usually represent only nominal values. Hence the individual identification of the particular motor is virtually mandatory.

Therefore we proposed an in-application off-line identification technique for BLDC motor parameters estimate. This technique does not require any additional hardware modification or a special measuring procedure since it is performed by a micro-controller in the target application.

But anyway, also other identifications techniques were used by various authors. For example, on-line identification of parameters using the Kalman filter in [7] or the recursive least-squares algorithm in [8] and [9]. And the last but not least - adaptive solutions such as [10].

A. Electrical parameters

The first step of the identification process is the stator winding electrical parameters estimate i.e. resistance $R[\Omega]$, and inductances for both axes $L_d[H], L_q[H]$.

Notice, that the BEMF observer, as described in the section V-A, can not operate without the knowledge of the concerned electrical parameters, hence neither the PLL and thereby the Park transform can not be evaluated yet.

1) *Aligning the rotor*: Since we do not know the initial position of the rotor, it has to be moved to the specific position first. By aligning the rotor we demand the following steady state:

$$\phi^* = 0 \quad \omega^* = 0 \quad (52)$$

Fortunately, this mechanical state can be reached just by applying an appropriate input signal:

$$u_\alpha = u^* \quad u_\beta = 0 \quad (53)$$

Assuming an arbitrary initial rotor position ϕ_0 , the applied signal (53) can be “imaginary” transformed to the dq reference frame using the inverse Park transform (5) as:

$$u_d = u^* \cos(\phi) \quad u_q = -u^* \sin(\phi) \quad (54)$$

Substituting the consequently created current vector into the torque equation (13) one can realize, that the torque is generated only if the angular position is non-zero i.e. $\phi \neq 0$. Thereby the proposed voltage signal (53) has an “aligning effect” to the rotor regardless of the initial position ϕ_0 .

If the rotor is correctly aligned and steady, then the Park transform (4) is equal to the identity matrix.

$$v_{dq} = v_{\alpha\beta} \quad (55)$$

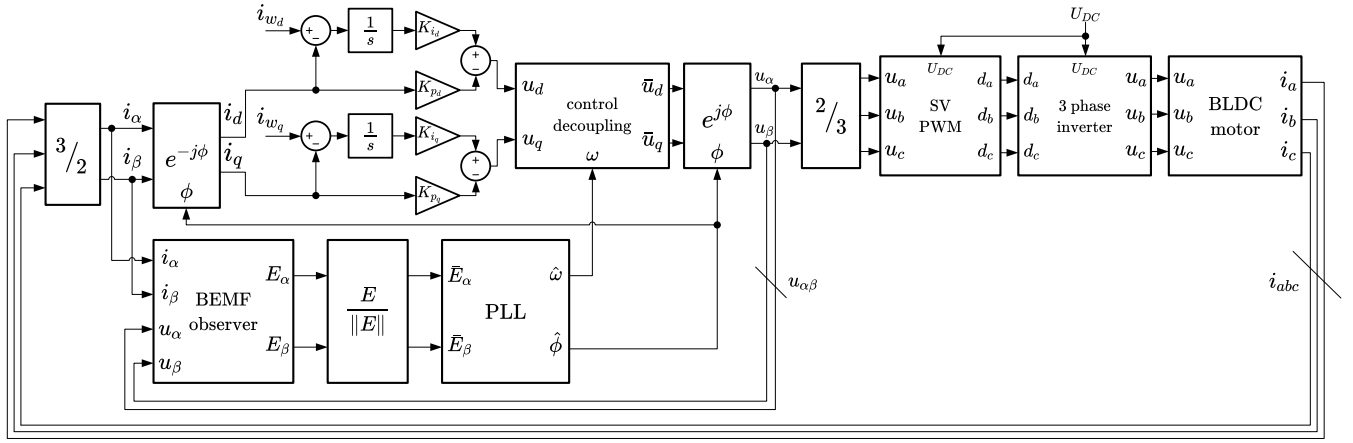


Fig. 5: Sensor-less field-oriented control scheme

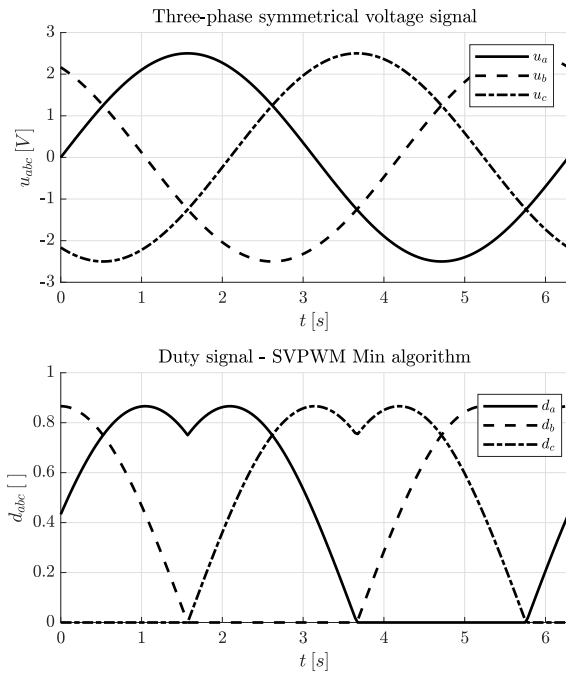


Fig. 6: SVPWM algorithm

2) *Transfer function model*: Assuming the steady state (52) as well as the consequent vector equivalence (55), the following transfer function models can be derived from the full models (11),(12):

$$\frac{i_{\alpha/\beta}(s)}{u_{\alpha/\beta}(s)} = \frac{1}{L_{d/q}s + R} \quad (56)$$

However, the whole process of identification is performed in discrete time domain so discrete equivalents of the models (56) have to be used.

$$\frac{i_{\alpha/\beta}(z)}{u_{\alpha/\beta}(z)} = \frac{b_{1\alpha/\beta}z^{-1}}{1 + a_{1\alpha/\beta}z^{-1}} \quad (57)$$

Parameters of the above discrete transfer function can be estimated using the least-squares method for the equivalent ARX model representation.

3) *ARX model identification*: The dynamic equation of the ARX model is defined as:

$$A(z^{-1})y(k) = B(z^{-1})u(k) + \epsilon(k) \quad (58)$$

Where ϵ stands for the exogenous random disturbance signal and u denotes the system input i.e. stator voltage component $u_{\alpha/\beta}$. The model output y , representing the stator current component $i_{\alpha/\beta}$, can be expressed in the vector form:

$$y(k) = h_{(k)}^T \theta + \epsilon(k) \quad (59)$$

The parameters vector θ :

$$\theta = [b_{1\alpha/\beta}, a_{1\alpha/\beta}]^T \quad (60)$$

The regression vector $h(k)$:

$$h(k) = [u_{(k-1)}, -y_{(k-1)}]^T \quad (61)$$

For the parameters estimate we prefer the off-line identification approach over on-line methods since these can not be performed in real-time for the demand of relatively small sample time.

The estimated output vector \hat{y} and the estimate residuals e for the measured output vector y are defined as:

$$\hat{y} = H\theta \quad e = y - \hat{y} \quad (62)$$

For N measurements, each row of the H matrix is defined as:

$$H_i = h_{(i)}^T \quad i = 1 \dots N \quad (63)$$

The parameters estimate $\hat{\theta}$ minimizing the sum of squared residuals $e^T e$ can be obtained by solving:

$$H^T H \hat{\theta} = H^T y \quad (64)$$

Both models for d and q axis have to be identified separately that way. For the q axis especially, the issue of consequent motor torque generation may arise. This torque might dis-align the rotor and the results would be biased. Therefore the length of the excitation signal has to be short enough (compared to the mechanical time constant) for this effect to be negligible.

Having the discrete transfer functions (57) identified, the estimated motor parameters can be finally determined. The stator resistance parameter estimate \hat{R} is equal to the mean of static gains reciprocal:

$$\hat{R} = \frac{1}{2} \left(\frac{1 + a_{1\alpha}}{b_{1\alpha}} + \frac{1 + a_{1\beta}}{b_{1\beta}} \right) \quad (65)$$

The stator inductance parameter estimate \hat{L} is related to the time constant of the system. Using the discrete-continuous time pole transform theorem one can write:

$$\hat{L}_{d/q} = -T_s \frac{\hat{R}}{\ln(-a_{1\alpha/\beta})} \quad (66)$$

B. Permanent magnetic flux estimate

The second step of the BLDC motor electrical parameters identification is the estimation of the constant magnetic flux $\psi_f [Vs]$ generated by the permanent magnet.

Analysing the dq reference frame model equations (11),(12), one can realize that the ψ_f parameter is related to a non-zero angular speed ω . Therefore to identify this parameter, the motor has to be running i.e. the whole FOC algorithm depicted in figure 5 must be applied.

Since the magnitude of the BEMF signal is linear to the angular speed ω and to the parameter ψ_f as defined in the equation (19), the least-squares method can be conveniently used for the ψ_f estimate.

The following linear regression system (62) can be formed:

$$y = [||E_1||, ||E_2||, \dots, ||E_N||]^T \quad (67)$$

$$H = [|\omega_1|, |\omega_2|, \dots, |\omega_N|]^T \quad (68)$$

The parameters vector becomes scalar in this case i.e. $\theta = \psi_f$.

VIII. TEST DEVICE AND IMPLEMENTATION

For verification of the proposed algorithms and assumptions presented in this paper, a real motor identification and control experiment was finally carried out. The subject of identification and control was a small-sized out-runner type BLDC motor with all the parameters unknown.

As a hardware platform we used the *STM32F446RE* (180 MHz, 512 KB Flash, 128 KB SRAM) micro-controller embedded in the evaluation board *Nucleo* along with the inverter extension board *X-NUCLEO-IHM11M* stacked on. The stator currents were measured using the single-shunt sensor topology and were sampled by the on-chip 12-bit analog-digital converter.

All the mentioned algorithms were implemented in the C++ programming language. Time-critical operations i.e. sensorless FOC loop were executed with the highest priority in the interrupt handle function of the timer. Other non-time-critical operations such as parameters identification and control synthesis were executed in separate tasks under management of the real-time operating system.

A. Experiment results

Sample-time for the identification and control experiment was chosen as $T_s = 27500^{-1} s$. The step-like two-level signal was applied as the excitation voltage signal for both axes during the identification process.

The resulting measured response of the system is shown in the figure 7. The following identified electrical parameters were obtained:

$$\hat{R} = 2.1574 \Omega \quad \hat{L}_d = 0.5478 mH \quad \hat{L}_q = 0.6215 mH \quad (69)$$

The simulated responses of the obtained continuous models $i_{d/q}^{sim}$ are also plotted in the figure 7 for results validation.

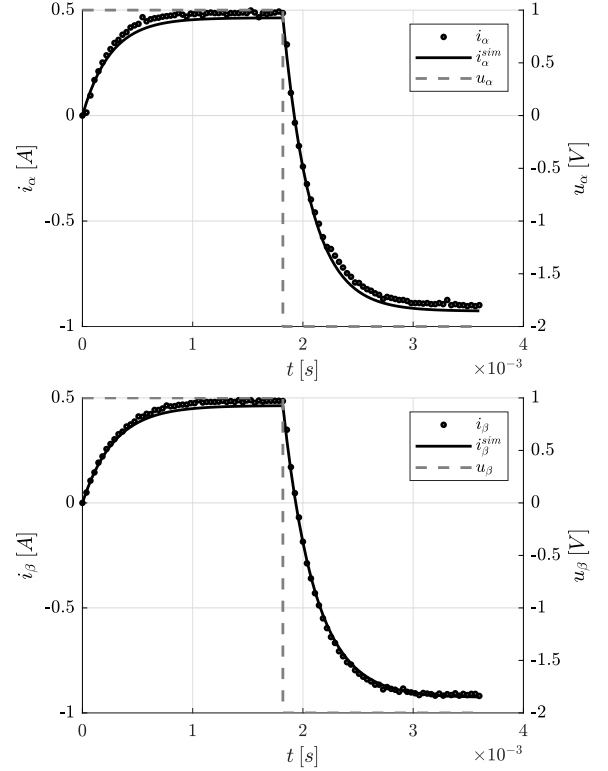


Fig. 7: Measured identification responses of $i_{\alpha,\beta}$ currents to input voltage signals $u_{\alpha,\beta}$

For the control algorithm, we have chosen the desired time constants (28) of the closed loop as:

$$T_1 = 20.0 ms \quad T_2 = 0.2 ms \quad (70)$$

By performing some empirical tuning, we found appropriate desired eigenvalues (42) for the BEMF observer as:

$$\lambda_{1,2} = -20.0 \times 10^3 \pm 5.0 \times 10^3 i \quad (71)$$

For the PLL we have chosen different eigenvalues:

$$\lambda_1^{PLL} = -100 \quad \lambda_2^{PLL} = -400 \quad (72)$$

Saturation settings (32),(33) for current controllers reflected the demand for greater dynamic range of quadrature component control.

$$\gamma = \frac{4}{5} \quad \delta = \frac{3}{5} \quad (73)$$

For the constant magnetic flux estimate, the values of $\|E_i\|$ and $|\omega_i|$ were asynchronously acquired to the assumed sample time of $T_s = 0.1$ s.

During this experiment, the FOC algorithm was operating for step-wise change of the quadrature current set-point $\Delta i_{q_w} = 0.15$ A resulting into desired motor acceleration. Thereby a variety of points was obtained during the identification as can be seen in the figure 8.

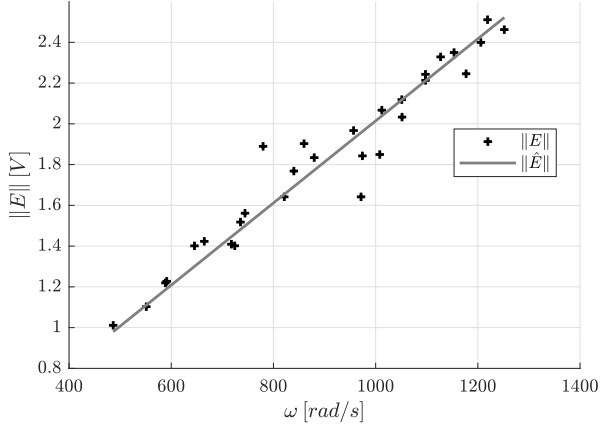


Fig. 8: Measured BEMF signal magnitude $\|E\|$ as a linear function of angular speed ω

Finally, the ψ_f parameter was estimated as:

$$\hat{\psi}_f = 0.00201[V s] \quad (74)$$

The control experiment was carried out for zero direct axis current set-point $i_{d_w} = 0$ and step-wise change of the quadrature axis current set-point $i_{q_w} = 0.1 \rightarrow 0.25$ A.

The acquired control data, plotted in the figure 9, proven the aperiodic behaviour of the closed control loop. As expected, the resulting angular speed of rotor ω correlated with the signal of the quadrature current i_q and changes in the quadrature axis current set-point were followed by the rotor (de)acceleration.

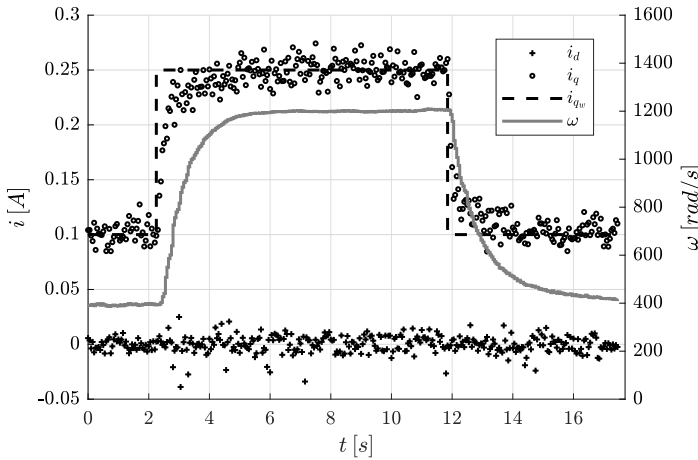


Fig. 9: Control of stator currents i_d, i_q for step-wise change of reference quadrature current i_{q_w}

IX. CONCLUSION

In this paper we introduced several improvements and modifications of commonly used algorithms and techniques concerning the BLDC motor sensor-less field-oriented control. The most significant work was made on developing the complex technique for the motor parameters identification, thereby a completely unknown motor can be easily controlled. This allowed us to apply the “plug and play” concept directly to an arbitrary controller-motor couple in practice. For the numeric realisation of the crucial vector-rotation operation we proposed the weighted Taylor series expansion as a replacement for traditional lookup tables. The FOC structure was modified by the IP controllers while considering constraints of the manipulated variables. We proposed the modification of the anti-windup algorithm with individual weighting of the voltage-vector components. Concerning the structure and design of the PLL, the concept of the Luenberger observer was exploited in order to replace the original PI-like estimators. Also other problems were treated in a new way - for example simple yet effective implementation of the SVPWM algorithm.

ACKNOWLEDGEMENT

This publication was created thanks to support under the Operational Program Integrated Infrastructure for the project: *International Center of Excellence for Research on Intelligent and Secure Information and Communication Technologies and Systems - II. stage*, ITMS code: 313021W404, co-financed by the European Regional Development Fund

REFERENCES

- [1] M. Žalman, *Akčné Čteny*, ser. Edícia skript / Slovenská technická univerzita. Slovenská technická univerzita, 2003.
- [2] S. Chen, X. Zhang, X. Wu, G. Tan, and X. Chen, “Sensorless control for ipmsm based on adaptive super-twisting sliding-mode observer and improved phase-locked loop,” *Energies*, vol. 12, p. 1225, 03 2019.
- [3] M. B. Astik, P. Bhatt, and B. R. Bhalja, “Analysis of sensorless control of brushless dc motor using unknown input observer with different gains,” *Journal of Electrical Engineering*, vol. 68, no. 2, pp. 99 – 108, 28 Mar. 2017.
- [4] Yongchang Zhang and Jiali Liu, “An improved q-pll to overcome the speed reversal problems in sensorless pmsm drive,” in *2016 IEEE 8th International Power Electronics and Motion Control Conference (IPEMC-ECCE Asia)*, 2016, pp. 1884–1888.
- [5] T. Erfidan, S. Urgun, Y. Karabag, and B. Cakir, “New software implementation of the space vector modulation,” vol. 3, 2004, pp. 1113–1115 Vol.3.
- [6] S. Tuncer and Y. Tatar, “A new approach for selecting the switching states of svpwm algorithm in multilevel inverter,” *European Transactions on Electrical Power*, vol. 17, no. 1, pp. 81–95, 2007.
- [7] O. Scaglione, M. Markovic, and Y. Perriard, “On-line parameter estimation for improved sensorless control of synchronous motors,” in *2012 XXth International Conference on Electrical Machines*, 2012, pp. 2229–2237.
- [8] S. J. Underwood and I. Husain, “Online parameter estimation and adaptive control of permanent-magnet synchronous machines,” *IEEE Transactions on Industrial Electronics*, vol. 57, no. 7, pp. 2435–2443, 2010.
- [9] E. B. Siqueira, J. L. Mor, R. Z. Azzolin, and V. M. de Oliveira, “Algorithm to identification of parameters and automatic re-project of speed controller of bldc motor,” *IFAC-PapersOnLine*, vol. 48, no. 19, pp. 256 – 261, 2015, 11th IFAC Symposium on Robot Control SYROCO 2015.
- [10] M. Tárnik and J. Murgaš, “Model reference adaptive control of permanent magnet synchronous motor,” *Journal of Electrical Engineering*, vol. 62, no. 3, pp. 117 – 125, 01 May. 2011.

ELITECH`21

23rd Conference of Doctoral Students

Faculty of Electrical Engineering and Information Technology

May 26, 2021



PROGRAM & REVIEW COMMITTEE

Chair: Eva Miklovičová

Vladimír Goga
Vladimír Jančárik
Ján Kardoš
Alena Kozáková

Máriuš Pavlovič
Danica Rosinová
Vladimír Šály
Martin Weis

ORGANIZING COMMITTEE

Chair: Alena Kozáková

Jana Paulusová, Ľubica Stuchlíková, Vladimír Šály, Elemír Ušák, Tomáš Váry

EDITOR

Alena Kozáková
Počet kusov: 20

CONFERENCE SUPPORTERS



Published by the Slovak University of Technology in Bratislava
in the SPEKTRUM STU Publishing, 2020

SPEKTRUM
STU

ISBN 978-80-227-5098-1

CONTENTS

Session I

MECHATRONIC SYSTEMS I

Chair: prof. Ing. Danica Rosinová, PhD.

1. IoT Edge Container with Artificial intelligence for Speech Recognition
Lukáš Beňo and Rudolf Pribiš - **Cena dekana**
2. Evaluation of open tools for designing and deploying Industry 4.0 Component based on Administration Shell
Rudolf Pribiš and Lukáš Beňo - **Cena IEEE**
3. Optimization of material flow in industrial warehouses
Filip Žemla, Ján Cigánek and Danica Rosinová - **Ocenenie SSKI**
4. Innovative Applications of Virtual and Augmented Reality for Industry and Services
Roman Leskovský, Erik Kučera, Oto Haffner, Dominik Janecký and Lea Lapšanská

Session II

MECHATRONIC SYSTEMS II

Chair: doc. Ing. Vladmír Goga, PhD.

1. Watt's centrifugal governor for DC motor
Ladislav Šarkán and Vladimír Goga
2. Lithium-ion battery modeling and SOC estimation methods - **Cena dekana**
Martin Baťa and Martin Sedláček
3. Methods of determining the position of the object in the field of view of the camera
Frederik Valocký, Peter Drahoš and Oto Haffner - **Ocenenie SSKI**
4. Vehicle model identification
Dávid Mikle, Martin Baťa and Juraj Račkay - **Cena IEEE**

Session III

Robotics & Cybernetics

Chair: doc. Ing. Ján Kardoš, PhD.

1. Improvements for BLDC motor control
Martin Dodek and Eva Miklovičová - **Cena dekana**
2. Gesture control for force compliant robotic manipulator
Marek Čorňák
3. Designing Human-Machine Interface for UAVs in structured environment using ROS and Flask
Filip Stec and Jozef Rodina - **Cena IEEE**
4. Simulation of a potential field obstacle avoidance method for UAV navigation
Adam Trizuljak and Jozef Rodina - **Ocenenie SSKI**

Session IV

ELECTRICAL POWER ENGINEERING

Chair: prof. Ing. Vladimír Šály, PhD.

1. The course of renewable resources production
János Kurcz, Anton Beláň, Vladimír Šály, Milan Perný - **Cena dekana**
2. Harmonisation of the requirements for electricity generators in the EU
Ján Poničan, Matej Sadloň and Marek Mokrání - **Cena IEEE**
3. The problem of far-field goniophotometry in lighting design
Marek Mokrání, Matej Sadloň and Ján Poničan

Session V

NUCLEAR POWER ENGINEERING

Chair: prof. Ing. Márius Pavlovič, PhD.

1. ALLEGRO as a demonstrator of GFR technology
Slavomír Bebjak
2. Determination of neutron flux distribution in structural components of EBO V2 reactor.

Michal Šnír, Kristína Krištofová, Gabriel Farkaš, Peter Hausner and Vladimír Slugeň
3. Comparison of the most commonly used scintillation detectors
Branislav Stríbrnský nad Róbert Hinca - **Cena IEEE**
4. BIM-based digital nuclear decommissioning support system
Dušan Daniška, Istvan Szóke and Franz Borrmann
5. Radiation protection calculations in the vicinity of the workplace for pumping sludge into barrels
Dávid Bednár, Martin Lištjak and Vladimír Nečas - **Cena dekana**
6. Calculation of ex-core detector spatial weight functions for reactor VVER-440
Peter Hausner and Gabriel Farkas
7. Criticality Safety Analysis of Wet Interim Storage Pool Using Monte Carlo Method
Katarína Kaprinayová and Gabriel Farkas

Session VI

ELECTRICAL ENGINEERING

Chair: prof. Ing. Vladimír Jančárik, PhD.

1. Effect of torso inhomogeneities on significance of ECG electrodes for forward and inverse problem
Beata Ondrušová and Jana Švehlíková - **Cena dekana**
2. An advanced software tool for analysis of experimental data obtained by Magnetic Adaptive Testing (MAT) Method
Lenka Hrušková and Elemír Ušák
3. Multifunctional hysteresis loop and Barkhausen noise recorder
Karol Hilko - **Cena IEEE**

Session VII

ELECTRONICS & PHOTONICS

Chair: prof. Ing. Martin Weis, DrSc.

1. Impact of different solutions on electrical parameters of CuO transistors ..
Tomáš Vincze, Michal Mičjan, Jaroslav Kováč and Martin Weis - **Cena IEEE**
2. Precharge circuit based on SiC transistor in linear mode for high voltage battery powered system
Michal Minárik and Juraj Marek - **Cena dekana**
3. Review of techniques for calibration of analog ICs
David Maljar, Michal Šovčík and Viera Stopjaková
4. Comparative Study of On-chip Inductive DC-DC Step-up Converters
Robert Ondica and Viera Stopjaková